RF and DC Power Handling Characterization of Thin Film Resistors Embedded on LCP

George E. Ponchak[1], Jennifer L. Jordan[1], Stephen Horst[2], and John Papapolymerou[2]
1. NASA Glenn Research Center, 21000 Brookpark Rd., Cleveland, OH 44135
George.ponchak@ieee.org, tel: 216-433-3504
2. School of Electrical and Computer Engineering, Georgia Institute of Technology, 85 Fifth Street NW, Atlanta, GA 30308

Abstract

For the first time, the DC and RF power handling capability of NiCrAlSi thin film resistors on Liquid Crystal Polymer (LCP) is presented. It is shown that there is a maximum power that the resistors can handle without causing degradation of the resistors, and this value is significantly less than the power required for burn out of the resistors. EDAX shows that the resistors fail due to electromigration of Ni and Cr, and migration of C from the LCP.

Introduction

Liquid Crystal Polymer (LCP) substrates are currently being used for packaging of microwave and millimeter wave circuits [1] [2] and as flexible substrates for antenna arrays [3] [4]. In each of these applications, embedded thin film resistors are required for bias circuits, power dividers, and loads. Thin film resistors on LCP have been reported, with their equivalent circuit models derived [5] [6], their use in power dividers demonstrated [7], and their use as attenuators demonstrated [8].

In many applications, large RF and DC power is required. For example, MEMS switches as reported in [4] require typical bias voltages of 50 V, and if the MEMS switch has extra stress, the bias voltage may be as high as 100 V. Ideally, no current is drawn when the capacitive switch is open or closed, but if a switch fails, a large DC current may flow through the bias resistors. Antenna arrays are typically used for radar, and high RF power is usually desired to increase sensitivity. If the antenna array incorporates MMIC power amplifiers, the DC power consumption of the amplifier can be very high. For example, a wide bandgap transistor based amplifier can draw between 4 and 24 W. Thus, the thin film embedded resistors on LCP should be characterized to determine their RF and DC power characteristics. To the best of our knowledge, thin film embedded resistors have not been characterized.

In this paper, thin film resistors embedded in a coplanar waveguide (CPW) structure [5] are characterized. First, the measured DC and RF resistance as a function of resistor length is presented, followed by the variation in resistance as a function of DC and RF power. Finally, the maximum DC and RF power that may be placed across the resistors and the variation in DC resistance as a function of temperature are discussed.

Description of Resistors

The fabrication and description of the resistors is found in [5]. Therefore, only a short description is given here. The resistors are formed by sputtering NiCrAlSi onto 0.5 oz. Cu sheets that are then laminated onto one side of a 0.004 inch thick LCP (ε_r=3.16) [9] using a heat press. The CPW lines and resistors are defined using a two step etching process. First, the CPW lines are defined by etching the Cu layer. This is followed by a second wet etch to remove the unwanted NiCrAlSi and define the resistors. Note that in this process, NiCrAlSi remains where the resistors exist and under all of the Cu areas of the circuit.

The CPW center conductor and slot widths are 250 and 300 μm, respectively. The test circuits are one port, CPW lines terminated by resistors formed between the center conductor and ground planes. There is no back side metal ground plane. Five resistors are characterized with their dimensions given in Table I and defined in Fig. 1.

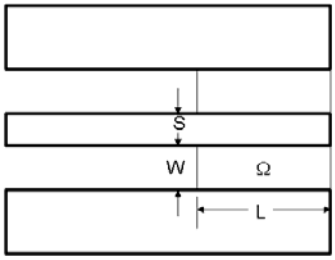

Figure 1: Schematic of CPW resistor.

Table 1: Dimensions of resistors.

	Length, L, (μm)	Width, W, (μm)	Area (mm^2)
R1	75	300	0.045
R2	150	300	0.090
R3	300	300	0.180
R4	600	300	0.360
R5	1200	300	0.720

Measurement Procedure

For all tests, a specially built, high temperature RF probe station is used [10]. The LCP substrate rests on a ceramic heater that is mounted on a piece of ceramic with a very low thermal conductivity. This thermally isolates the LCP substrate during tests at room temperature and permits characterization as a function of temperature without changing the test bench. Because thin, flexible LCP is being proposed for deployable arrays that will be thermally isolated, it is believed that these test conditions closely approximate the actual usage conditions.

For the DC resistance tests, a 650 μm pitch, ground-signal-ground RF probe is used to contact the CPW. A bias T is connected directly to the RF probe to provide the voltage or current to the resistor, with the other RF port of the bias T terminated in a 50 Ω load. An Agilent parameter analyzer is used to sweep the voltage and measure the current. The current limit is set to 500 mA to allow the device to draw high

currents when it starts to fail. Note that sweeping the current and measuring the voltage prevents or delays the resistor from failing, which gives an optimistic estimate of power handling capability. Calibration is performed by measuring the resistance when the probe is placed on a Cu short circuit. This resistance is subtracted from all subsequent measurements. All measurements are performed at least two times, and the results averaged.

For the RF characterization at 2.5 GHz using a CW source, the same 650 μm pitch probe is used to contact the CPW, however, no bias T is required. A four port network analyzer is used to measure the reflection coefficient of the CPW resistor. A TWT power amplifier increases the RF power from the network analyzer, and couplers are used to sample the input and reflected signal, both of which are fed back to the network analyzer. An open-short-load calibration at the probe tip is performed at an input power of 10 dBm. The electrical length of the CPW feed line is determined by measuring the characteristics of an open circuit terminated line of the same length, again at 10 dBm. This electrical length is mathematically subtracted from subsequent measurements to place the reference plane at the resistor. In addition, a coupler is used after the TWT amplifier to measure the power with a power meter. The insertion loss of the cables, couplers, and attenuators in the path to the RF power meter was measured and this value is used to correct the RF input power values. All RF measurements are repeated a minimum of three times and the reported results are the average of those measurements.

Measured Resistance

The measured resistance at DC and 2.5 GHz is shown in Fig. 2. It is seen that the variation in resistance between DC and 2.5 GHz is approximately 15%, but both curves follow the expected $R=\rho W/tL$ relationship where t is the resistor thickness, ρ is the material resistivity, and W and L are defined in Figure 1.

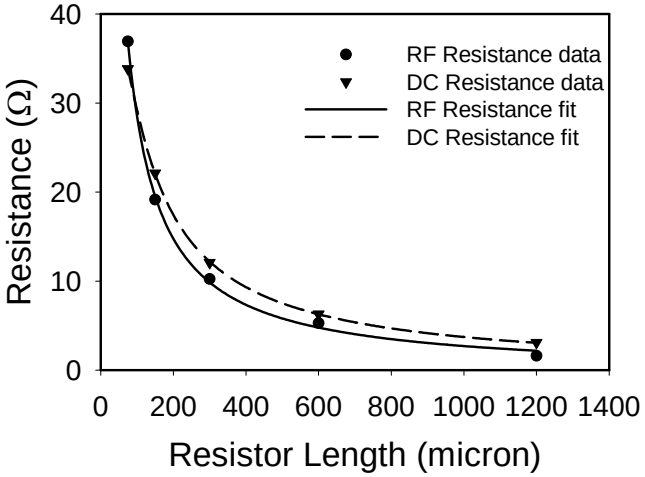

Figure 2: Measured resistance as a function of resistor length, L.

DC Power Handling Capability

Because manufacturing variations cause variations in the characteristics of resistors of the same nominal length, the results are normalized by dividing by the DC resistance at the lowest power level. Figure 3 shows a typical variation in resistance with DC power level (it is for the shortest length resistor). It is seen that the resistance increases almost linearly with DC power until a certain power that we call P_{max} is reached. DC power greater than P_{max} causes the resistance to decrease and the resistor to fail. Typically, the resistors failed as open circuits. The significance of P_{max} is explored further with RF power handling capability in the next section. The resistor was cycled through power levels lower than P_{max} with a short time interval of less than 30 seconds and a longer wait between cycles of 5 minutes, and the resistor values did not vary greater than the measurement error.

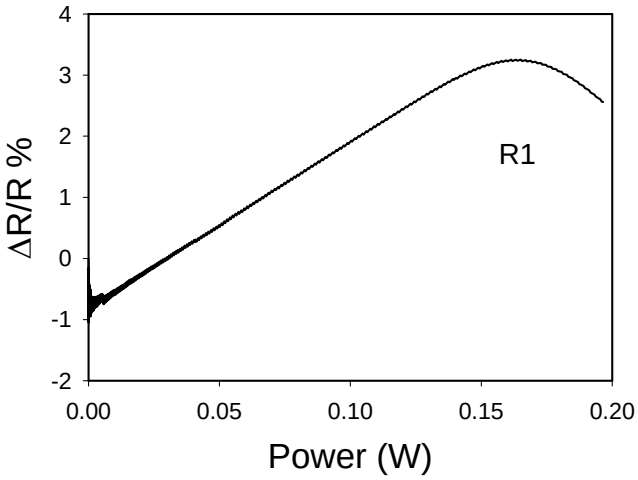

Figure 3: Measured variation in resistance as a function of DC power.

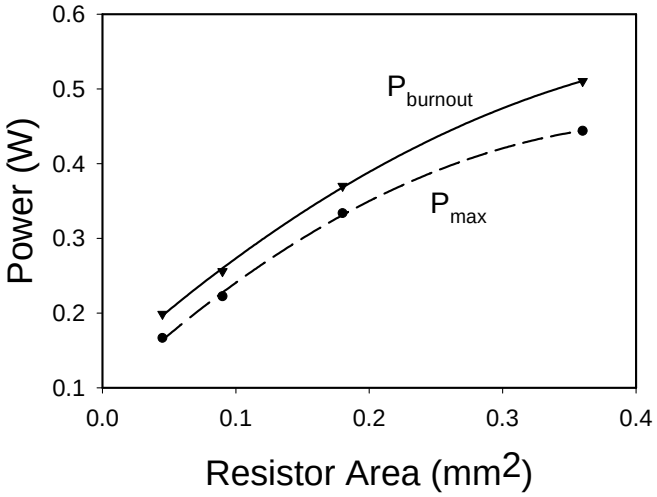

Figure 4: Measured DC power for burnout and P_{max} as a function of resistor area.

Figure 4 shows the DC power required for burnout and P_{max} as a function of the resistor area. It is observed that the power handling capability of the resistor increases with resistor area. It is also seen that P_{max} and $P_{burnout}$ have a similar dependency on area. Figure 5 shows the DC power density handling capability as a function of resistor area. Both of these curves agree with the general results for NiCr resistors embedded in microstrip lines on FR4 boards, thus showing that the results are not dependent on the resistor layout.

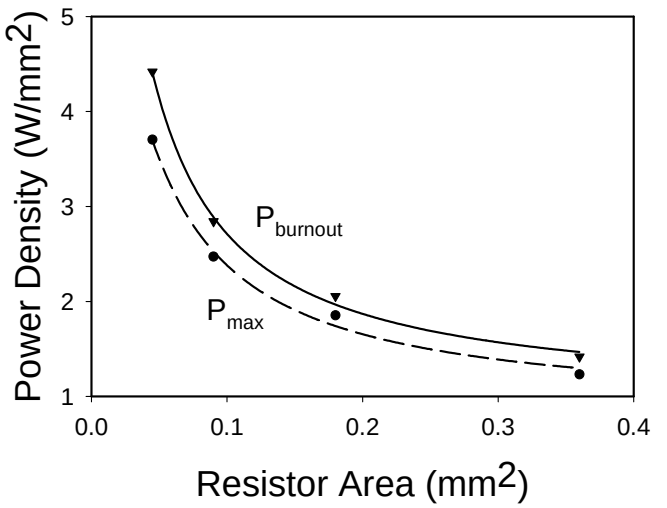

Figure 5: Measured DC power density for burnout and P_{max} as a function of resistor area.

RF Power Handling Capability

The RF power handling capability of the resistors is measured at 2.5 GHz. Figure 6 shows the change in resistance and inductance as a function of the RF power. It is seen that the resistance increases with RF power until a value that shall be called P_{RFmax}, after which the change in resistance decreases with RF power. A similar observation is made about the change in reactance. Although not shown, it was observed that at P_{RFmax} and higher powers, the resistance is unstable and decreases with time. If the power is swept above P_{RFmax}, the resistance decreases until the resistor burns out. Furthermore, if the power is cycled above P_{RFmax}, the resistance is observed to permanently decrease as shown by curves labeled Run 1, 2, and 3 in Fig. 6a. Each of these curves is for the same resistor that is cycled from a low power to a power greater than P_{RFmax}. In Figure 6a, the symbols labeled Run 4 are for a resistor that is cycled three times to a power lower than P_{RFmax}. It is observed that if the power is kept below P_{RFmax}, the resistance is stable. Thus, it is inferred that material changes occur at P_{RFmax}.

Figure 7 shows P_{RFmax} and the burn out power as a function of resistor area. Figure 8 shows the power density at P_{RFmax} and $P_{burnout}$ as a function of resistor area. The RF power handling capabilities follow the same trend as the DC power handling capability. It is also observed in Fig. 7 that resistors must be backed off at least 3 dBm from the burnout power for stable, reliable operation.

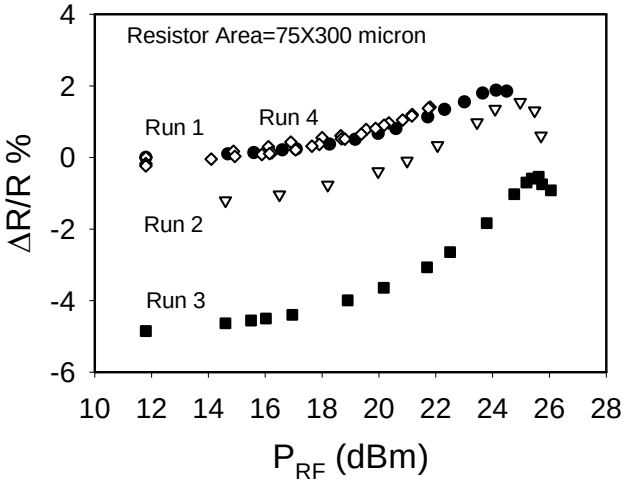

(a)

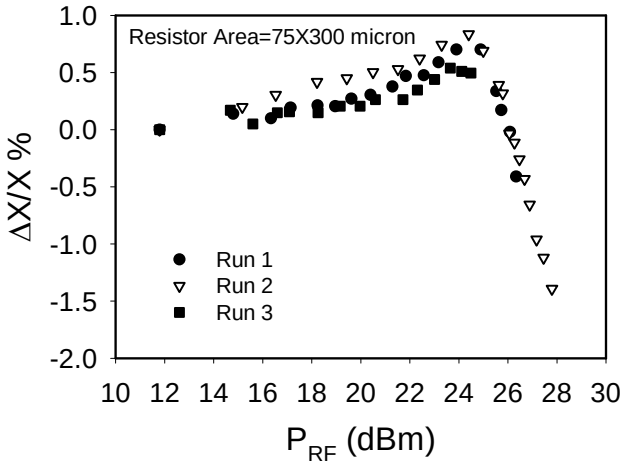

(b)

Figure 6: Change in (a) resistance and (b) reactance as a function of RF power at 2. 5 GHz. (Run 1, 2, and 3 are for the same resistor cycled through a P_{RF} greater than P_{RFmax}. Run 4 is for the same resistor cycled through a P_{RF} less than P_{RFmax}.)

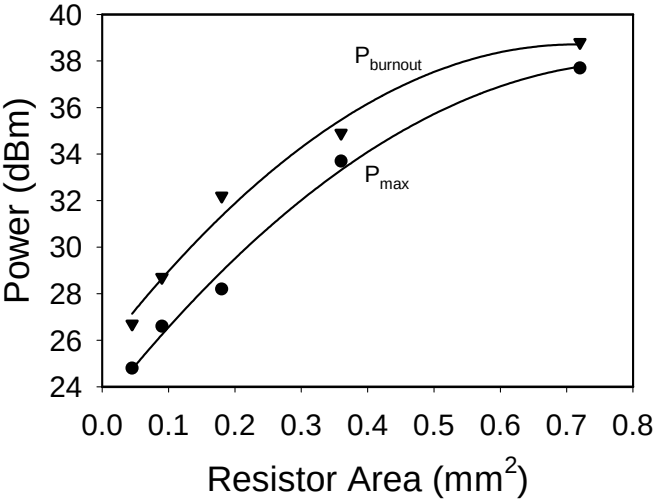

Figure 7: Burnout RF power and maximum RF power as a function of resistor area.

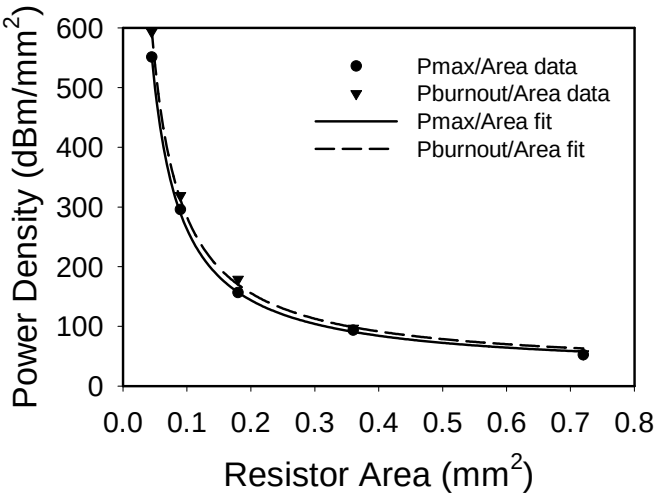

Figure 8: Power density of P_{RFmax} and $P_{burnout}$ versus resistor area.

Temperature Coefficient of Resistance

The DC resistance of the resistors is measured as a function of temperature by placing the LCP on a ceramic heater and cycling the temperature from 25 to 125˚ C. Figure 9 shows the change in resistance as a function of temperature. It is seen that the change in resistance is less than 2 percent for all but the lowest value resistor.

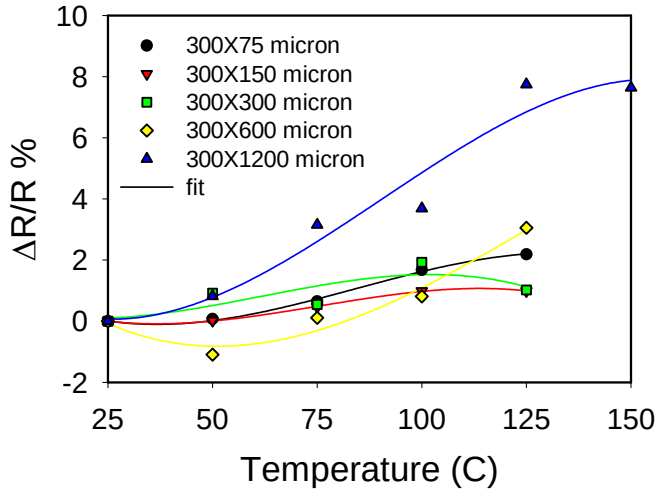

Figure 9: Change in resistance as a function of temperature.

Failure Analysis

Microphotographs of the resistors after failure due to excess DC and RF power were obtained for each resistor. Figure 10 shows photographs of a resistor that failed due to excess DC power. It is observed that the failure occurs uniformly across the resistor at a point where there is a minimum in the resistor width due to fabrication errors and, thus, higher current density and therefore greater heating. All resistors that failed due to excess DC power had similar failure characteristics, with blistering of the metal resistor. Figure 11 shows the same sized resistor after excess RF power. It is observed that failure occurs along the edges of the resistor where there is higher RF current density. All resistors that failed due to excess RF power had similar characteristics.

Semi-quantitative energy dispersive spectrometry (EDS) measurements of the concentration of materials show that the failure is initially due to electromigration of the Ni and Cr. Especially notice the resistor on the right side of Fig. 11b where a lack of metal is seen. In this region, NiCr migration from the edges of the resistor towards the center is apparent. After further heating due to DC or RF power, the LCP starts to melt under the resistor and C migrates upwards from the LCP, thus causing the blistering of the resistor. Note that the LCP melts at 285 C. Analysis shows that there is a high concentration of C and a lower concentration of Ni and Cr in the resistors after failure. Thin film resistors on GaAs have shown a similar sequence of electromigration with first a movement of NiCr and then migration of Ga from the GaAs [12]. A single resistor cycled 3 times to 3 dB less RF power than P_{max} (Run 4 in Fig. 6a) was also shown to have reduced Ni and Cr and higher C than an unstressed resistor. Thus, even though a measurable change in resistance is not shown in Fig. 6a, it is apparent that the resistor has been overly stressed. Therefore, for reliable resistor characteristics, resistors should be backed off at least 3 dB from P_{max}, or 6 dB from $P_{burnout}$.

As noted earlier, the resistors fail as open circuits. Examination of Figs. 10b and 11b show breaks in the metallization due to electromigration and the upward blistering of the resistor, which causes the thin film resistor to tear.

Conclusions

Thin film resistors on Liquid Crystal Polymer (LCP) have good temperature stability and predictable resistance. However, they must not be used to burnout. From the data taken for this small set of resistors, the DC power should be backed off 40% from $P_{burnout}$ and the RF power should be backed off 6 dB from $P_{burnout}$ for reliable operation.

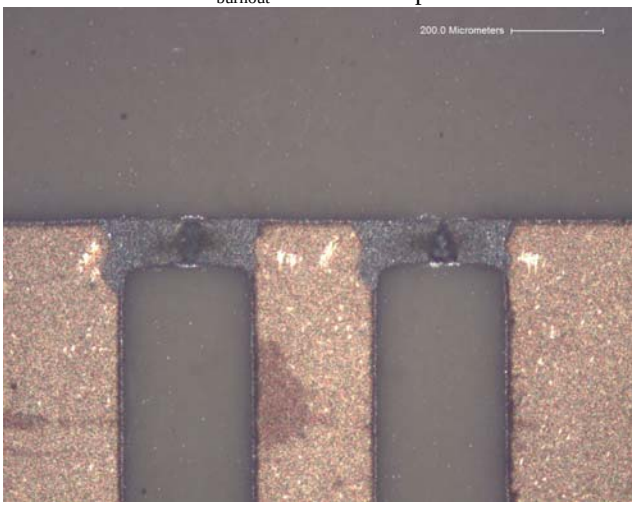

(a)

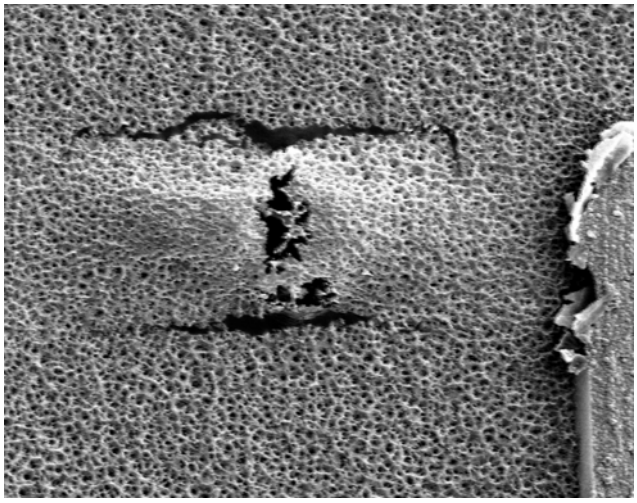

(b)

Figure 10: Photograph and microphotograph of resistor that failed due to excessive DC power.

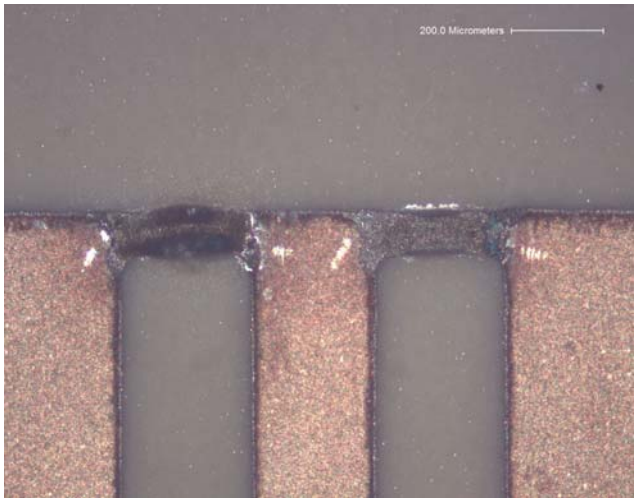

(a)

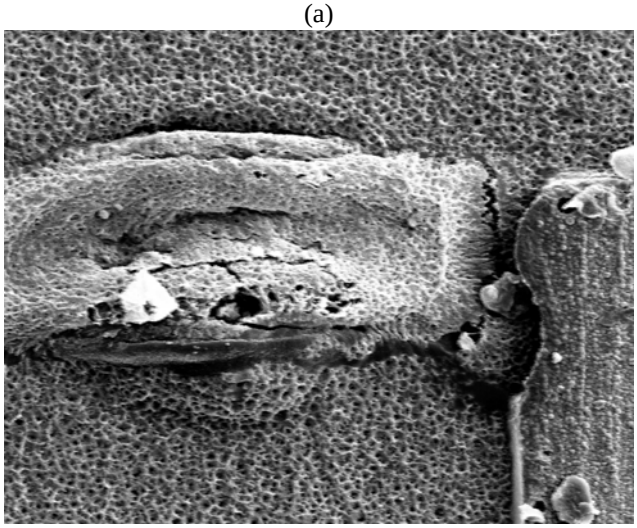

Figure 11: Photograph and microphotograph of resistor that failed due to excessive RF power.

Acknowledgements

The authors would like to acknowledge the help of Mr. Nicholas Varaljay for performing the EDAX analysis and the NASA ESTO ROSES program for funding assistance.

References

1. D.C. Thompson, M.M. Tentzeris, and J. Papapolymerou, "Packaging of MMICs in multilayer LCP substrates," *IEEE Microwave and Wireless Components Letters*, Vol. 16, Issue 7, July 2006, pp. 410 – 412.
2. Z. Wei, and A. Pham, "Liquid crystal polymer (LCP) for microwave/millimeter wave multilayer packaging," *IEEE MTT-S Int. Microwave Symposium Dig.*, June 8-13, 2003, pp. 2273 – 2276.
3. G. DeJean, R. Bairavasubramanian, D. Thompson, G.E. Ponchak, M.M. Tentzeris, and J. Papapolymerou, "Liquid Crystal polymer (LCP): a new organic material for the development of multilayer dual-frequency/dual-polarization flexible antenna arrays," *IEEE Antennas and Wireless Propagation Letters*, Vol. 4, 2005, pp. 22 – 26.
4. N. Kingsley, G.E. Ponchak, and J. Papapolymerou, "Reconfigurable RF MEMS phased array antenna integrated within a liquid crystal polymer (LCP) system-on-package," accepted to *IEEE Trans. on Antennas and Propagation*.
5. S. Horst, S. Bhattacharya, S. Johnston, M. Tentzeris, and J. Papapolymerou, "Modeling and characterization of thin film broadband resistors on LCP for RF applications," *Proc. Electronic Components and Tech. Conf.*, May 30-June 2, 2006, pp.1751-1755.
6. Gang Zou, H. Gronqvist, and Johan Liu, "Integrated Capacitors and Resistors on Liquid Crystal Polymer Substrate," *Conf. on High Density Microsystem Design and Packaging and Component Failure Analysis*, June 2005, pp. 1 – 4.
7. S. Horst, S. Bhattacharya, M. Tentzeris, and J. Papapolymerou, "Monolithic Low Cost Ka-Band Wilkinson Power Dividers on Flexible Organic Substrates," *Proc. Electronic Components and Technology Conf.*, May 29-June 1, pp. 1851 – 1854.
8. S. Horst, D.E. Anagnostou, G.E. Ponchak, E. Tentzeris, and J. Papapolymerou, "Beam-Shaping of Planar Array Antennas Using Integrated Attenuators," *Proc. Electronic Components and Tech. Conf.*, May 29-June 1, 2007, pp. 165 – 168.
9. D.C. Thompson, O. Tantot, H. Jallageas, G.E. Ponchak, M.M. Tentzeris, and J. Papapolymerou, "Characterization of liquid crystal polymer (LCP) material and transmission lines on LCP substrates from 30-110 GHz," *IEEE Trans. Microwave Theory and Tech*, Vol. 52 , No. 4 , pp. 1343 - 1352, April 2004.
10. Z. D. Schwartz, A. N. Downey, S. A. Alterovitz, and G. E. Ponchak, "High-temperature RF probe station for device characterization through 500 ° C and 50 GHz," *IEEE Trans. on Instrumentation*, Vol. 54, No. 1, pp. 369-376, Feb. 2005.

11. Jiangtao Wang, M. K. Davis, R. Hilburn, and S. Clouser, “Power dissipation of embedded resistors,” *2003 IPC Printed Circuits Expo*, Long Beach, CA, March 23-27, 2003.
12. C. Sydlo, K. Mutamba, L. Divac Krnic, B. Mottet, and H.L. Hartnagel, “Reliability studies on integrated GaAs power-sensor structures using pulsed electrical stress,” *Microelectronics Reliability*, Vol. 43, pp. 1929-1933, Oct. 2003.